Experimental and Numerical Investigation of Rarefied Interacting Plumes

Ivan A. Chirokov[*], Tatiana G. Elizarova[†], Jean-Claude Lengrand[**], Isabelle Gibek[‡] and Irina A. Graur[§]

[*]*Moscow State University, Department of Numerical Mathematics and Informatics, Moscow, Russia*
[†]*Institute of Mathematical Modeling, Russian Academy of Science, Moscow, Russia*
[**]*Laboratoire d'Aérothermique du CNRS, Orléans, France*
[‡]*Centre National d'Etudes Spatiales, Toulouse, France*
[§]*Institute of Mathematical Modeling Russian Academy of Science, Moscow, Russia*

Abstract. Experimental and numerical investigations of the interaction of two rarefied underexpanded parallel plumes and of the interaction of a plume with a parallel plate are presented. Numerical results are in a reasonable agreement with the experimental ones including the low-density far field. Results obtained give access to flow features not available from the measurements.

CONTEXT OF THE STUDY

Scientific and technological space missions using micro or mini-satellites are generating growing levels of interest. CNES developed new platforms for micro-satellites (satellites whose total launch mass is about 120 kg) and for mini-satellites (satellites whose total launch mass is about 500 kg). The platform for mini-satellites is called *PROTEUS* (Re-configurable Platform for Observation, TElecommunications and Scientific Uses). These platforms are designed to lower costs, so that it is possible to carry out a greater number of experiments. They will be valuable tools for space experimentation and for rapid demonstrations of the feasibility of new concepts. Their in-orbit lifetime will be about three years.

Plume effects. The propulsion subsystems of the micro-satellite platform (whenever propulsion is required) and of the mini-satellite platform are hydrazine propulsion subsystems. In particular, they consist of four thrusters whose thrust is one Newton at the beginning of the mission. The thrusters are all located on the same side of the satellite. As the satellites are small (side of about $1\,\text{m} \times 1\,\text{m}$ for a mini-satellite, side of about $0.6\,\text{m} \times 0.6\,\text{m}$ for a micro-satellite), the thrusters are very close one to another, which is unusual. During the satellite maneuvers, they are always activated at the same time. As far as plume effects are concerned, there is not any surface in front of the thrusters plumes. But a question has been raised: is there any risk of thermal or dynamic load, caused by the interactions of the plumes, for the surface on which the thrusters are located ? Indeed, sensitive equipment may be laid on this surface. That is why a study has been necessary. It started as an experimental work carried out in the SR3 low-density facility of the Laboratoire d'Aérothermique du CNRS on reduced-scale models that simulate real satellite configurations. It continued as a theoretical and numerical work to improve the prediction tools capable of treating the plume impingement problem.

Present work. A simplified configuration has been considered in the present work, consisting in two (instead of four) parallel plumes (twin plumes). The problem of a single plume interacting with a flat plate parallel to its axis has been also considered. It is very similar to the previous one because the flat plate replaces the symmetry plane of the twin plume configuration. For both problems, numerical results have been compared with available experimental results.

In the flow under consideration the pressure and density vary strongly from the nozzle exit section to the external parts of the plume. The cross section of the plume changes dramatically from 2 millimeters near the nozzle to several centimeters at the downstream limit of the computational domain. These features require the implementation of fine computational grids, as well as a large number of iterative steps for convergence. In order to minimize computational

time, the numerical algorithm has been implemented for a powerful multiprocessor computational system.

Computations were carried out based on the quasigasdynamic equations. Computational results for twin plumes were discussed in [1].

EXPERIMENTAL SETUP

Nitrogen jets were issued from one or two parallel conical nozzle(s) that simulated satellite control thrusters. The twin plumes (type I) were issued from a 15-degrees half-angle conical nozzle with critical radius $r_c = 0.2$ mm, stagnation conditions $T_0 = 900$ K and $p_0 = 12$ bars. The single plume (type X) was issued from a 7-degrees half-angle conical nozzle with the same critical radius, stagnation conditions $T_0 = 1100$ K and $p_0 = 16$ bars. The distance between parallel axes of jets I was 50 mm and the distance between the axis of jet X and the flat plate, parallel to it, was 17 mm. Experimental investigations consisted in determining flowfield density by means of electron beam surveys and in wall pressure measurements ([2]–[5]).

Flow conditions and gas parameters corresponding to the experimental results are given in Table 1. They were used for the numerical simulation. Subscript $_e$ corresponds to the conditions at nozzle exit, $_\infty$ corresponds to the background gas, $_w$ refers to wall conditions. Ma denotes the Mach number, r_e - the nozzle exit radius, λ - the mean free path, Kn - the Knudsen number ($Kn_e = \lambda_e/(2r_e)$), $\gamma = 1.4$ - the specific heat ratio, $Pr = 14/19$ - the Prandtl number.

TABLE 1. Flow parameters

	Jet I	Jet X
r_e (m)	$1.6 \cdot 10^{-3}$	$1.7 \cdot 10^{-3}$
λ_e (m)	$1.304 \cdot 10^{-6}$	$1.397 \cdot 10^{-6}$
Kn_e	$4.07 \cdot 10^{-4}$	$4.1 \cdot 10^{-4}$
Ma_e	5.781	5.813
T_e (K)	117.1	141.8
p_e (Pa)	954	1230
u_e (m/s)	1275	1411
p_∞ (Pa)	1	1
$T_\infty = T_w$ (K)	293	293

QUASIGASDYNAMIC EQUATIONS

The numerical calculation is based on the QuasiGasDynamic (QGD) system of equations. QGD equations can be obtained using the Boltzmann equation in BGK approximation (e.g. [6], [7]) and also using a traditional phenomenological approach, where gasdynamic quantities (density ρ, velocity u_i, pressure p and temperature T) are defined as time- space average quantities [8], whereas for the Navier-Stokes model, these quantities are defined as space averaged ones. A review of theoretical and numerical results for QGD equations can be found in [9]. According to [8], the QGD equations form a system of three partial-derivative equations accounting for conservation of mass (continuity equation)

$$\frac{\partial \rho}{\partial t} + \nabla_i J^i = 0, \tag{1}$$

conservation of momentum

$$\frac{\partial (\rho u^k)}{\partial t} + \nabla_i J^i u^k + \nabla^k p = \nabla_i \Pi^{ik}, \tag{2}$$

and conservation of total energy

$$\frac{\partial E}{\partial t} + \nabla_i \frac{J^i}{\rho}(E + p) + \nabla_i q^i = \nabla_i (\Pi^{ik} u^k). \tag{3}$$

The total volumic energy is $E = 0.5\rho u_i^2 + p/(\gamma - 1))$.

To close the system (1)–(3), the mass flux vector J^i, the shear-stress tensor Π^{ik}, and the heat flux vector q^i must be expressed as a function of macroscopic flow quantities. The particular QGD system is obtained by taking

$$J^i = \rho u^i - \tau \left(\nabla_j(\rho u^i u^j) + \nabla^i p \right), \tag{4}$$

$$\Pi^{ik} = \Pi^{ik}_{NS} + \tau u^i \left(\rho u^j \nabla_j u^k + \nabla^k p \right) + \tau g^{ik} \left(u_j \nabla^j p + \gamma p \nabla_j u^j \right), \tag{5}$$

and

$$q^i = q^i_{NS} - \tau \rho u^i \left(u^j \nabla_j \varepsilon + p u_j \nabla^j (\frac{1}{\rho}) \right). \tag{6}$$

Here q^i_{NS} and Π^{ik}_{NS} are the Navier-Stokes heat flux and shear-stress tensor, g^{ik} is the metric tensor, $\varepsilon = p/(\rho(\gamma - 1))$, $p = \rho RT/M$. The parameter τ is an averaging time equal to $\tau = (\gamma \mu)/(Sc \rho a^2)$, where μ is the viscosity coefficient, a is the sound velocity and Sc is the Schmidt number. For a perfect gas $Sc \approx 1$, $a^2 = \gamma RT/M$, and $\tau = \mu/p$ is the Maxwell relaxation time, that is close to the mean time between successive molecular collisions.

For the QGD equations, mass, momentum, total energy conservation laws and the entropy theorem are valid as for the classic Navier-Stokes system. QGD and Navier-Stokes systems differ in the order of $O(\tau)$. For stationary flows the dissipative terms (terms in τ) in the QGD equations have the asymptotic order of $O(\tau^2)$ for $\tau \to 0$, or in the dimensionless form of the equations, $O(Kn^2)$ for $Kn \to 0$. The boundary layer approximation for QGD equations leads to the classical Prandtl equation system.

For modeling rarefied hypersonic flows QGD equations have some advantages compared with Navier-Stokes ones, especially for constructing numerical algorithms (e.g. [7] - [9]).

PROBLEM FORMULATION AND NUMERICAL ALGORITHM

The problems for twin jet interactions and for the interaction of a jet with parallel plate are solved in (x, y, z) cartesian formulation. The single jet is regarded in (r, z) formulation.

The viscosity law is taken as $\mu \sim T^\omega$, ω being related to intermolecular interaction. For nitrogen N_2 we take $\omega = 0.75$. The parameter τ is taken equal to μ/p, which ensures that the Navier-Stokes and QGD dissipation terms are consistent and allows to obtain the QGD equations in compact form as e.g. in [7].

Slip boundary conditions were used for the vertical solid wall to the left of the nozzle exit section and for the plane (horizontal solid wall). "Soft" conditions were used for the downstream boundary. The background pressure was imposed on the lateral boundaries. At the nozzle exit section a laminar inflow boundary layer profile was prescribed. For 3D computations the symmetry conditions were used to reduce the number of space grid nodes. Additional information can be found in [10].

Numerical modeling of the jet flow is based on a finite-difference algorithm. The computational domain is covered with a rectangular non-uniform space grid. QGD equations are approximated by the finite-difference centered scheme. In order to stabilize the numerical solution an artificial dissipation of the order of $O(\beta h)$ is added to the dissipative terms, except the terms with mixed space derivatives ($\partial/\partial x_i \partial/\partial x_j, i \neq j$). The length h represents the space grid step. For the variants under consideration β is taken in the range $0.1 - 1$. This procedure may be regarded as a variant of the vector-splitting approach.

The finite-difference scheme is solved by an explicit algorithm where the steady-state solution is attained as the limit of a time-evolving process. The choice of the time step is based on the stability condition in the form $h_t = \alpha \min(h/a)$.

Calculations have been performed on a cluster multiprocessor computer system with distributed memory equipped with 24 Intel Pentium III microprocessors. This system is located in the Laboratoire d'Aérothermique. The Message Passing Interface (MPI) standard has been used to organize the interprocessor data exchange. Parallel code is constructed using a domain decomposition technique (geometrical parallelism). This means that the whole computational domain is divided into subdomains in the jet axis direction and each processor provides for calculations in its own subdomain. Efficiency estimations show that the implemented numerical algorithm (explicit in time and homogeneous in space approximation of QGD equations) allows an efficient implementation on cluster multiprocessor systems.

Algorithm modification for the rarefied flows In the construction of macroscopic equations (NS as well as QGD ones) a development on the small parameter τ (in dimensionless form on the Knudsen number Kn) near the Maxwellian

distribution function is used. When Kn becomes sufficiently large, the macroscopic models lose their validity. In jet-flow computations, this effect results in an non physical increase of gas temperature in the jet far field.

For QGD equations, a solution to this problem can be introduced as follows : during the computations the value of τ is monitored within the flowfield. If τ exceeds some characteristic value τ_0, then it is forced to the value τ_0. Otherwise it is calculated as usual as $\tau = \mu/p$. This limitation of τ occurs in regions characterized by a rather large value of Bird's parameter $(P = \lambda/(\rho/\nabla\rho))$, where the continuum description of the flow is questionable.

For the calculations presented here, τ was taken equal to μ/p (realistic viscosity) or limited to its value τ_e at nozzle exit.

COMPUTATIONAL RESULTS

Computations were carried out for flow conditions corresponding to the experiment (Table 1). The computational results are divided into two groups:

- single jet X (r,z formulation) and the interaction of jet X with a parallel plate (x,y,z formulation).
- twin parallel jets I (x,y,z formulation).

Dimensionless quantities were introduced based on nozzle exit gas parameters. However the computational results are presented in usual dimensional form. The computed number density was normalized by the stagnation number density ($n_0 = 1.054 \times 10^{26}\,\mathrm{m}^{-3}$ for jet X, $n_0 = 9.657 \times 10^{25}\ \mathrm{m}^{-3}$ for jets I).

For jet X in r,z formulation the computational grid was 260×130. For jet X in cartesian formulation the grid was $140 \times 42 \times 62$, the x-direction step $h_x = r_e = 1.7\,\mathrm{mm}$, y- and z-directions minimal step $h_y = h_z = r_e/2 = 0.85\,\mathrm{mm}$. For jets I the computational grid ($N_x \times N_y \times N_z$) was $140 \times 43 \times 74$, the x-direction step was $h_x = r_e = 1.6\,\mathrm{mm}$, y- and z-directions minimal steps were $h_y = h_z = r_e/2 = 0.8\,\mathrm{mm}$. In all cases h_y and h_z increased between adjacent cells by a constant factor 1.05 outside the nozzle exit section.

For 3D problems the number of time steps to achieve the converged solution was of the order of 10^4–10^5, which took about 10 hours machine time of 8 Pentium III processors, working in parallel. A detailed description of the computational results can be found in [10].
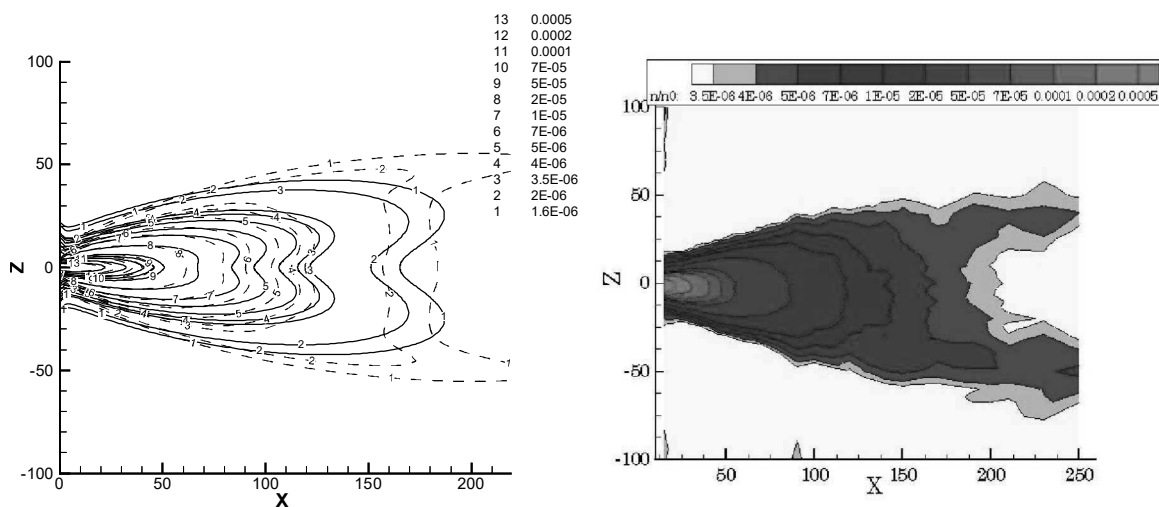

FIGURE 1. Calculated (left) and measured (right) density contours for single jet

Results for jet X

Fig. 1 represents the calculated number density contours in the (r,z) formulation together with the experimental density contours [4]. Here the computational domain was doubled according to the symmetry axis conditions. This

variant was used to check the grid convergence of the numerical algorithm (4 computation grids were used) and to check the dependence of the numerical solution on the limitation of τ.

The solution with $\tau = \mu/p$ is shown by dashed lines, the numerical results for the restricted $\tau = \tau_e = \mu_e/p_e$ is shown by solid lines. Both calculated density contours match well the experimental ones in the inner part of the jet and are not sensitive to the limitation of τ used. However density profiles for $\tau = \mu/p$ correspond better to the experiment in the far field, than the profiles for τ. But the jet temperature in the far field for non restricted τ value becomes unrealistically high. The choice $\tau = \tau_e$ provides lower temperature, and in 3D calculations τ was set equal to τ_e.

Fig. 2 represents the calculated number density contours in the $(x, y = 0, z)$ plane for the jet interaction with a parallel plate. The calculated contours match well the experimental ones [4]. The calculated velocity vectors indicate that there is no backward flow.

Fig. 3–4 depict calculated and measured transverse number density profiles. They are in good agreement with the experimental results [4].
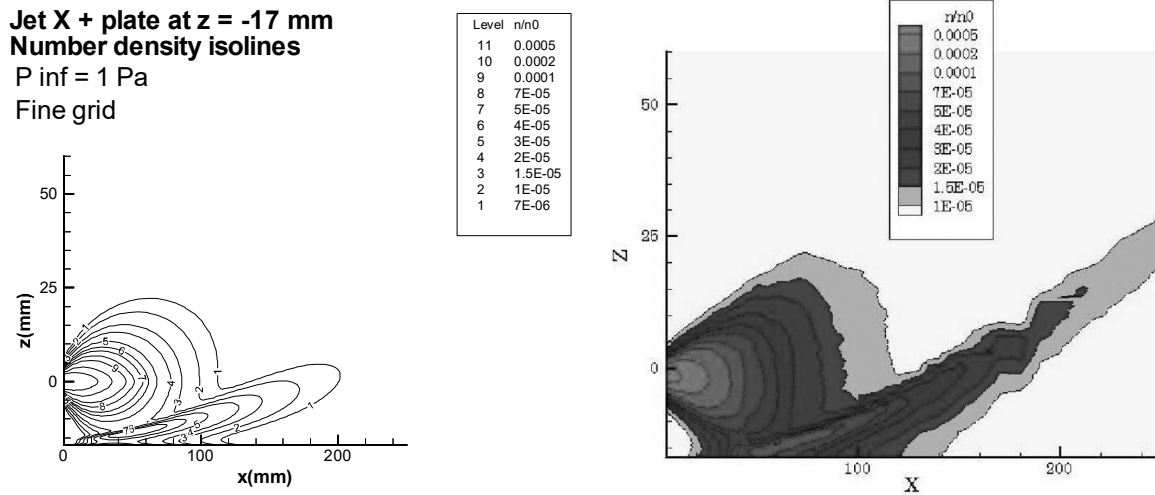
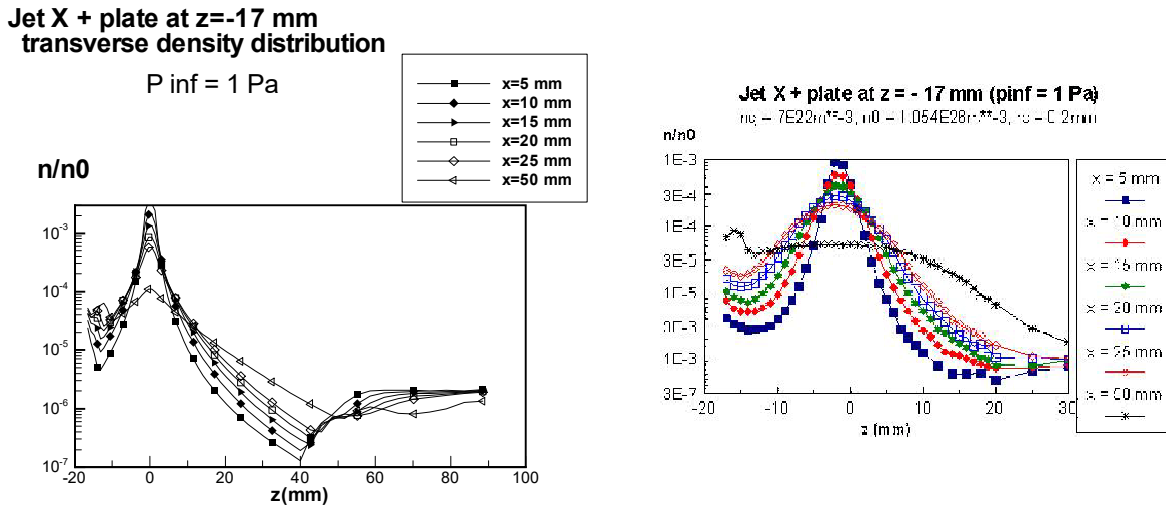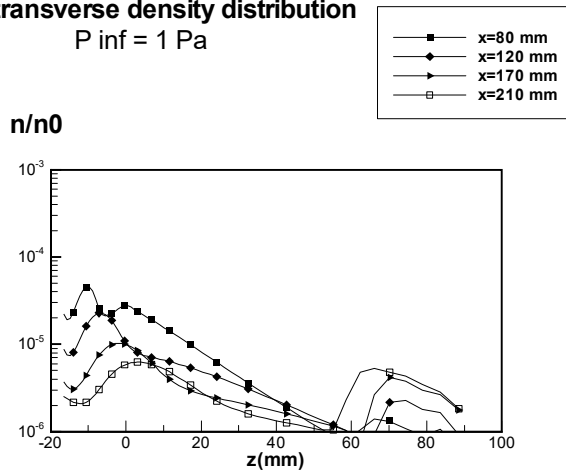**FIGURE 2.** Calculated (left) and measured (right) density contours for jet-plate interaction

FIGURE 3. Calculated (left) and measured (right) transverse density distribution, part1

Fig. 5 represents longitudinal ($z = -17$ mm, $y = 0$) and transverse ($x = 40$ mm, $z = -17$ mm) on-plate pressure profiles. They are compared with experimental results, taken from [5]. Refinement of the space grids makes the computational results closer to the experimental distributions.

Results for twin jets I

Fig. 6 represents the calculated and measured number density contours in the ($x, y = 0, z$) plane. On the figures the computational domain was doubled according to the symmetry plane conditions. In the present numerical results, the interaction between the jets begins at a distance x somewhat smaller than in the experiment. Except for this small difference, the calculated contours match well the experimental ones [2], [3], [4]. The calculated velocity vectors in the same plane do not reveal any backward flow.

FIGURE 4. Calculated (left) and measured (right) transverse density distribution, part2
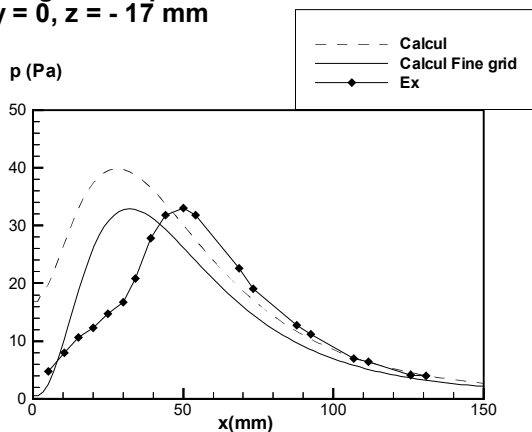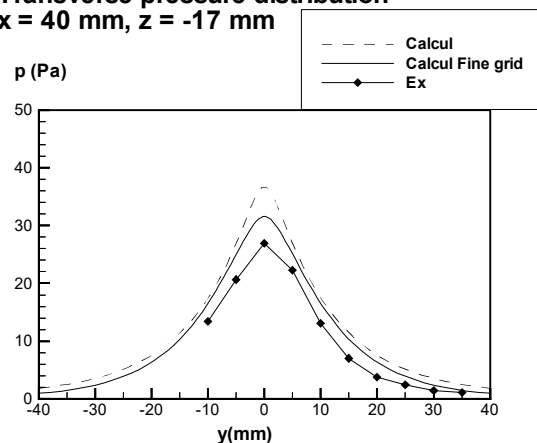
FIGURE 5. Longitudinal (left) and transverse (right) on-plate pressure profiles

Double jet I - number density isolines   P inf = 1 Pa

Level	n/n0
10	0.0003
9	0.00015
8	7E-05
7	3E-05
6	2E-05
5	1.5E-05
4	1E-05
3	7E-06
2	5E-06
1	3E-06
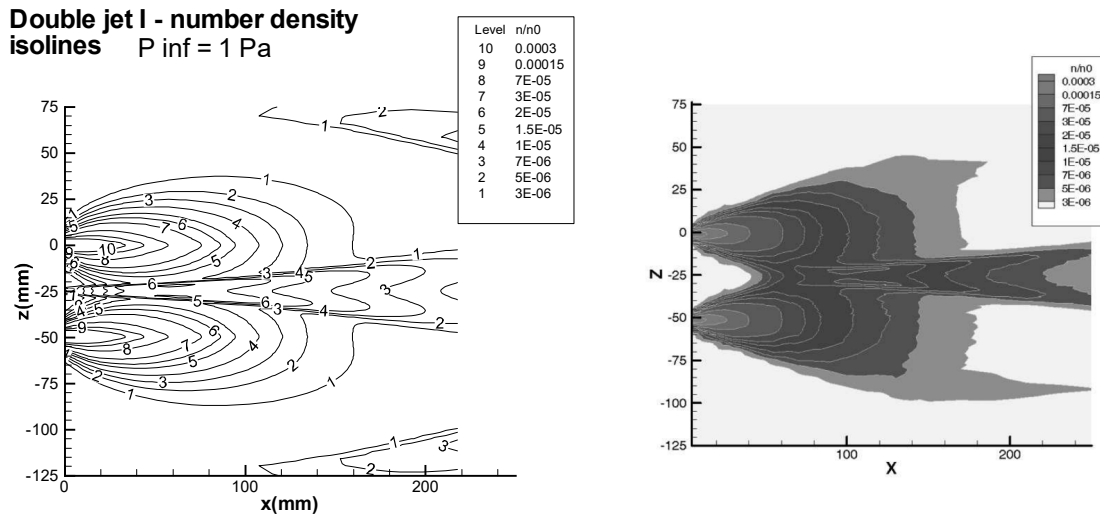
FIGURE 6.   Calculated (left) and measured (right) density contours

Double jet I - transverse density distribution

P inf = 1 Pa

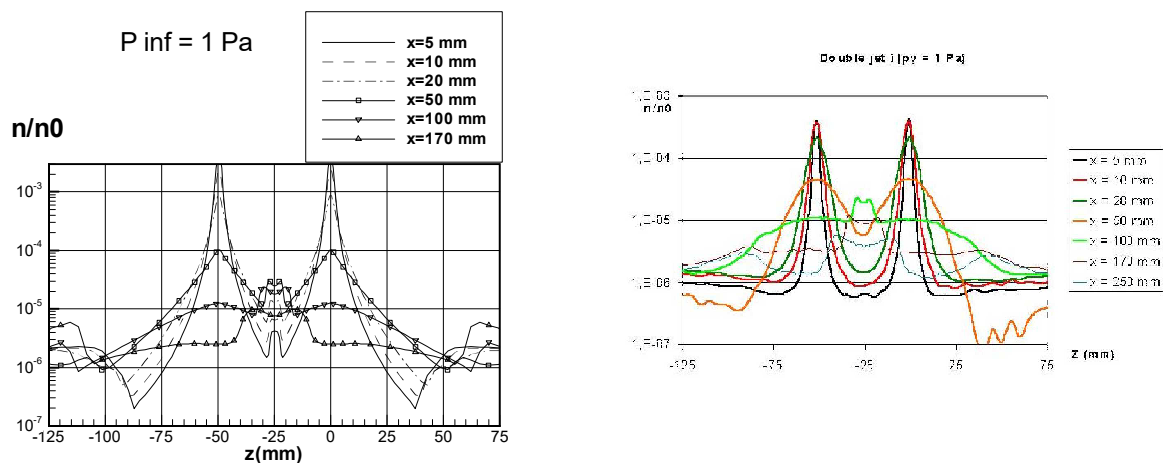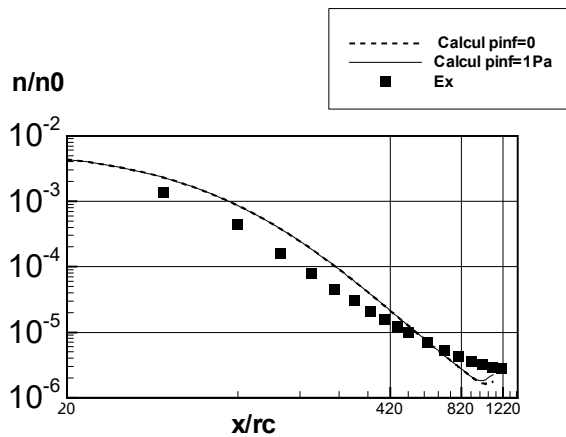|	
———	x=5 mm
– – –	x=10 mm
–·–·–	x=20 mm
–□–	x=50 mm
–▽–	x=100 mm
–△–	x=170 mm

n/n0

FIGURE 7.   Calculated (left) and measured (right) transverse density distributions

Fig. 7 represents transverse number density profiles. They are in good agreement with the experimental results [3], [4].

Fig. 8 represent on-axis values ($z = 0. y = 0$) for number density and for Mach number. They are compared with experimental results taken from [3], or [4]. x is normalized by $r_c = 0.2$ mm. The density distribution is close to the experimental one. The jet interaction is visible at large abscisses on numerical results, whereas it does not yet appear in the experimental results. For the large abscisses the calculated values of the Mach number are smaller then those estimated from the experiments using a Pitot tube. The discrepancy occurs in a domain where the gas temperature is only a few Kelvin and the Mach number values are not significant because of strong translational nonequilibrium, which affects the Pitot pressure measurements.

Double jet I - axial density distribution   **Double jet I - axial Mach number distribution**
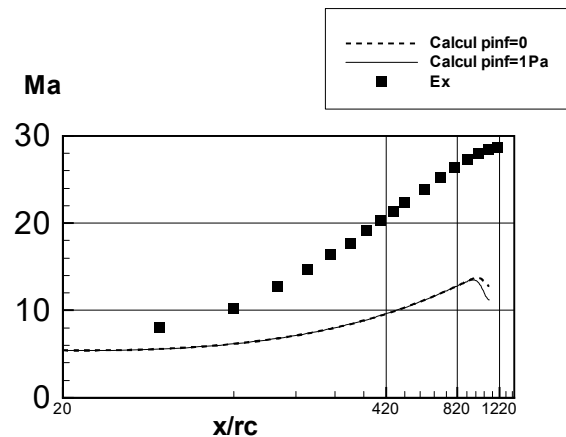

FIGURE 8.   Axial density (left) and Mach number (right) distributions

CONCLUSION

The experimental and numerical investigation of the interaction of two rarefied underexpanded parallel plumes and the plume interaction with a parallel plate have been presented. Numerical results correspond to the experimental ones including the density contours for the external low-density parts of the jets. On-plate density and pressure distributions also match well the measurements.

Numerical results provide information on those quantities not measured in the experiment, e.g. the absence of a recirculation zone between twin jets and in the jet-plane configuration.

REFERENCES

1. Chirokov I.A., Elizarova T.G., Gibek I., Lengrand J.-C.: Numerical and experimental investigation of interacting plumes. Proc. 4th Europ. Symp. Aerothermodynamics for Space Applications, ESA SP-487, pp. 381–388, 2002.
2. Allègre J., Lombardo G., Lengrand J.-C.: Interaction entre deux jets et une paroi de satellite. Lab. d'Aérothermique du CNRS, RC 99-1, Janv.1999.
3. Allègre J., Chaix A., Lengrand J.-C.: Etude expérimentale de la densité dans des jets sous-détendus. Lab. d'Aérothermique du CNRS, NT 99-1, Sep.1999.
4. Allègre J., Chaix A., Gorchakova N.G., Purpura C., Lengrand J.-C.: Etude expérimentale de jets propulsifs issus de tuyères parallèles. Lab. d'Aérothermique du CNRS, RC 2000-1, Sep.2000.
5. Allègre J., Bisch D., Lengrand J.-C.: Impact de jets sur des parois: Mesures de pression et visualisations. Lab. d'Aérothermique du CNRS, RC 96-1, Janv. 1996.
6. Chetverushkin B.N.: Kinetically-consistent finite-difference schems in gasdynamics. Moscow, MGU, 1999 (in russian).
7. Elizarova T.G., Lengrand J.-C., Graur I.A.: Gradient expansions for distribution functions and derivation of moment equations. 21th Intern. Symp.on Rarefied Gas Dynamics, Ed. R.Brun et al., Cepadues, Toulouse, France, 1999,Vol.1, pp.119–126.
8. Sheretov Yu.V.: Mathematical modeling of liquid and gas flows based on quasihydrodynamic and quasigasdynamic equations. Tver University, 2000 (in Russian).
9. Elizarova T.G., Sheretov Yu.V.: Theoretical and numerical investigation of quasigasdynamic and quasihydrodynamic equations. Comput. Mathem. and Mathem. Phys., 2001, V.41, No 2, pp. 219–234.
10. Graur I.A., Elizarova T.G, Chirokov I.A., Lengrand J.-C.: Calcul par une approche continue de jets sous-détendus, de leurs interactions mutuelles et de leurs interactions avec des parois. Lab. d'Aérothermique du CNRS, RC 2002 - 1, 2002.